

hep-ph/9612380
 Freiburg-THEP 96/23
 December 1996

Electroweak $\mathcal{O}(\alpha)$ Corrections to W^+W^- Pair Production in Polarized $\gamma\gamma$ Collisions

G. Jikia¹

*Albert-Ludwigs-Universität Freiburg, Fakultät für Physik
 Hermann-Herder Str.3, D-79104 Freiburg, Germany*

and

*Institute for High Energy Physics
 Protvino, Moscow Region 142284, Russia*

Abstract

Full $\mathcal{O}(\alpha)$ electroweak corrections for $\gamma\gamma \rightarrow W^+W^-$ are calculated including virtual corrections, soft and hard real photon and Z -boson emission. The corrections are quite large ranging from -2.5% at 500 GeV to -18% at 2 TeV, $|\cos\theta^\pm| < \cos(10^\circ)$. Contributions from real photon and Z -boson emission are important at high energies where they partly cancel large negative contribution originating from virtual bosonic corrections. Precision measurements that intend to uncover physics beyond the standard model must necessarily make use of the full standard model predictions including $\mathcal{O}(\alpha)$ corrections.

¹Alexander von Humboldt Fellow; e-mail: jikia@phyv4.physik.uni-freiburg.de

1. Introduction

A high-energy $\gamma\gamma$ linear collider, that can be obtained from Compton backscattered intense laser beams off electron linac beams [1–3] could be a very useful tool for studying the electro-weak symmetry breaking mechanism which is known as one of the last most important untested ingredients of the Standard Model (SM). In models with a light Higgs particle, one unique opportunity for $\gamma\gamma$ colliders relates to the production of the Higgs on resonance and its ability to perform a direct measurement of the $H\gamma\gamma$ coupling in the reactions $\gamma\gamma \rightarrow H \rightarrow b\bar{b}$, ZZ [4]. Another very interesting question concerns the observability of the Higgs boson signal in the reaction $\gamma\gamma \rightarrow WW$. In the case of very heavy mass Higgs boson $m_H \geq 1$ TeV, unfortunately, a huge background from transverse $W_T W_T$ continuum makes searches of the heavy Higgs signal in $\gamma\gamma \rightarrow W^+W^-$ hopeless [5–7]. However, for $m_H \sim (200 \div 300)$ GeV recently [8] it was mentioned that on the Higgs resonance the Born cross section $\gamma\gamma \rightarrow W^+W^-$, Breit-Wigner Higgs production cross section and the interference between these two processes are of the same order of magnitude in α . Moreover, a large destructive interference was found between the continuum and the s -channel Higgs exchange, so that Higgs boson would be manifested as a resonant dip in the WW invariant mass distribution. So, at least in principle, with excellent WW -mass resolution and high luminosity it will be possible to look for the signal of relatively light Higgs boson in this reaction.

If no light Higgs boson would be discovered at LEP2, LHC or the linear collider, the best strategy to probe the symmetry breaking sector would lie in the study of the self couplings of the W , Z bosons. The large cross sections for the processes involving W 's give $\gamma\gamma$ colliders an advantage in probing the self couplings. Indeed, the reaction $\gamma\gamma \rightarrow W^+W^-$ would be the dominant source of the W^+W^- pairs at future linear colliders, provided that photon-photon collider option will be realized. The Born cross section of W^+W^- pair production in photon-photon collisions in the scattering angle interval $10^\circ < \theta^\pm < 170^\circ$ is 61 pb at $\sqrt{s_{\gamma\gamma}} = 500$ GeV and 37 pb at 1 TeV. Corresponding cross sections of W^+W^- pair production in e^+e^- collisions are an order of magnitude smaller: 6.6 pb at 500 GeV and 2.5 pb at 1 TeV. With more than a million WW pairs per year a photon-photon collider can be really considered as a W -factory and an ideal place to conduct precision tests on the anomalous triple [9–11] and quartic [11–13] couplings of the W bosons. In addition, in the process of triple WWZ vector boson production it is possible to probe the tri-linear ZWW and quartic couplings [11, 13–15] as well as the C violating anomalous ZWW , γZWW interactions [15].

With the natural order of magnitude on anomalous couplings [17], one needs to know the SM cross sections with a precision better than 1% to extract these small numbers. From a theoretical point of view this calls for the need to calculate full $\mathcal{O}(\alpha)$ cross section of W^+W^- pair production in $\gamma\gamma$ collisions including radiative corrections and real photon and Z -boson emission.

In this paper we summarize our results [15, 16] for the complete $\mathcal{O}(\alpha)$ electroweak corrections taking into account one-loop electroweak virtual radiative corrections, soft and hard photon and Z -boson emission. Virtual and soft-photonic corrections to the process $\gamma\gamma \rightarrow W^+W^-$ have been also recently calculated by Denner, Dittmaier and Schuster [18]. We find complete agreement with the numerical results of Refs. [18].

The paper is organized as follows: In Section 2 we define the helicity amplitudes, discuss their symmetry properties and define all the independent helicity amplitudes. In Section 3 the tree-level cross sections for various polarizations in the high energy limit are considered. The general structure of $\mathcal{O}(\alpha)$ corrections is defined in Section 4. In Section 5 explicit analytical results for the leading contributions from heavy Higgs boson and top-quark are given. Also light fermion contributions and asymptotic behavior in the leading logarithmic approximation at high energy are discussed.

Numerical results are presented in Section 6.

2. The $\gamma\gamma \rightarrow W^+W^-$ helicity amplitudes

The helicity amplitudes for the reaction

$$\gamma(p_1, \lambda_1) + \gamma(p_2, \lambda_2) \rightarrow W^+(p_3, \lambda_3) + W^-(p_4, \lambda_4) \quad (2.1)$$

are defined as follows

$$\mathcal{M}_{\lambda_1\lambda_2\lambda_3\lambda_4} = e_1^{\mu_1}(\lambda_1)e_2^{\mu_2}(\lambda_2)e_3^{\mu_3*}(\lambda_3)e_4^{\mu_4*}(\lambda_4)G_{\mu_1\mu_2\mu_3\mu_4}(p_1, p_2, p_3, p_4), \quad (2.2)$$

where λ_i denotes the polarization of particle i . The momenta and polarization vectors for different helicities in the c.m.s. of the initial photons are given by

$$\begin{aligned} p_{1,2} &= E(1; 0, 0, \pm 1), \\ p_{3,4} &= -E(1; \pm \beta \sin \theta_W, 0, \pm \beta \cos \theta_W); \end{aligned} \quad (2.3)$$

$$\begin{aligned} e_1^{\pm} &= e_2^{\mp} = \frac{1}{\sqrt{2}}(0; \mp 1, -i, 0), \\ e_3^{\pm*} &= e_4^{\mp*} = \frac{1}{\sqrt{2}}(0; \mp \cos \theta_W, +i, \pm \sin \theta_W), \\ e_{3,4}^0 &= \frac{E}{M_W}(\beta; \pm \sin \theta_W, 0, \pm \cos \theta_W). \end{aligned} \quad (2.4)$$

All momenta are taken to be incoming. Here e^{\pm} is γ or W -boson polarization vector with transverse helicity ± 1 and e^0 is the polarization vector of the longitudinal W boson.

The helicity amplitudes are given by the sum of parity-even (\mathcal{A}) and parity-odd (\mathcal{B}) contributions. As bosonic vertices are P and C even, \mathcal{B} -contribution comes solely from fermion loop contribution.

$$\mathcal{M}_{\lambda_1\lambda_2\lambda_3\lambda_4}(s, t, u, \beta, p_T) = \mathcal{A}_{\lambda_1\lambda_2\lambda_3\lambda_4}(s, t, u, \beta, p_T) + \mathcal{B}_{\lambda_1\lambda_2\lambda_3\lambda_4}(s, t, u, \beta, p_T). \quad (2.5)$$

We show explicitly β and $p_T = E\beta \sin \theta_W$ as the arguments of the amplitudes. Taking into account the relations $\beta^2 = 1 - 4M_W^2/s$ and $p_T^2 = (tu - M_W^4)/s$ the amplitudes can be expressed as rational functions of Mandelstam variables s , t and u

$$s = (p_1 + p_2)^2, \quad t = (p_2 + p_3)^2, \quad u = (p_1 + p_3)^2. \quad (2.6)$$

and linear function of β , p_T and scalar loop four-, three-, two- and one-point functions D , C , B and A [23]. With definitions (2.3)–(2.4) the following relations take place

$$\mathcal{M}_{\lambda_1\lambda_2\lambda_3\lambda_4}(s, t, u, \beta, -p_T) = (-1)^{\lambda_3 + \lambda_4} \mathcal{M}_{\lambda_1\lambda_2\lambda_3\lambda_4}(s, t, u, \beta, p_T), \quad (2.7)$$

$$\mathcal{M}_{\lambda_1\lambda_2\lambda_3\lambda_4}(s, t, u, -\beta, p_T) = (-1)^{\lambda_3 + \lambda_4} \mathcal{M}_{\lambda_1\lambda_2\lambda_3\lambda_4}(s, t, u, \beta, p_T). \quad (2.8)$$

The helicity amplitudes are related by Bose symmetry, parity and charge conjugation

$$\text{Bose: } \mathcal{M}_{\lambda_1\lambda_2\lambda_3\lambda_4}(s, t, u, p_T) = \mathcal{M}_{\lambda_2\lambda_1\lambda_3\lambda_4}(s, u, t, -p_T), \quad (2.9)$$

$$\text{P: } \mathcal{A}_{\lambda_1\lambda_2\lambda_3\lambda_4}(s, t, u) = (-1)^{\lambda_3 + \lambda_4} \mathcal{A}_{-\lambda_1-\lambda_2-\lambda_3-\lambda_4}(s, t, u), \quad (2.10)$$

$$\text{C: } \mathcal{A}_{\lambda_1\lambda_2\lambda_3\lambda_4}(s, t, u, p_T) = \mathcal{A}_{\lambda_1\lambda_2\lambda_4\lambda_3}(s, u, t, -p_T). \quad (2.11)$$

P and C violating amplitudes \mathcal{B} acquire an additional minus sign under parity and charge conjugation transformations. At one-loop level CP is an exact symmetry of all the amplitudes even with complex Cabibbo-Kobayashi-Maskawa matrix. Taking into account the symmetry properties (2.7)–(2.11) all helicity amplitudes can be expressed through eight independent P -even helicity amplitudes \mathcal{A} and six independent P -odd helicity amplitudes \mathcal{B}

$$\begin{aligned}
\mathcal{A}_{++++}(\beta) &= \mathcal{A}_{+---}(-\beta); \\
\mathcal{A}_{+++-} &= \mathcal{A}_{++-+}; \\
\mathcal{A}_{++00}(\beta) &= \mathcal{A}_{++0+}(\beta) = -\mathcal{A}_{++0-}(-\beta) = -\mathcal{A}_{++-0}(-\beta); \\
\mathcal{A}_{++00}; \\
\mathcal{A}_{+-+-} &= \mathcal{A}_{+---}; \\
\mathcal{A}_{+-+-}(\beta) &= \mathcal{A}_{+--+}(-\beta); \\
\mathcal{A}_{+-+0}(\beta) &= \mathcal{A}_{+-0+}(-\beta) = -\mathcal{A}_{+-0-}(\beta) = -\mathcal{A}_{+--0}(-\beta); \\
\mathcal{A}_{+-00}; \\
\mathcal{B}_{++++} &= \mathcal{B}_{+++-} = \mathcal{B}_{++00} = 0; \\
\mathcal{B}_{+++-}(\beta) &= \mathcal{B}_{++-+}(-\beta); \\
\mathcal{B}_{++00}(\beta) &= -\mathcal{B}_{++0+}(\beta) = \mathcal{B}_{++0-}(-\beta) = -\mathcal{B}_{++-0}(-\beta); \\
\mathcal{B}_{+-+-} &= \mathcal{B}_{+---}; \\
\mathcal{B}_{+-+-}(\beta) &= \mathcal{B}_{+--+}(-\beta); \\
\mathcal{B}_{+-+0}(\beta) &= \mathcal{B}_{+-0+}(-\beta) = -\mathcal{B}_{+-0-}(\beta) = -\mathcal{B}_{+--0}(-\beta); \\
\mathcal{B}_{+-00}.
\end{aligned} \tag{2.12}$$

It is worth mentioning that tree level amplitudes are equal to zero for equal helicities of incoming photons and unequal helicities of final W 's

$$\mathcal{M}_{++LT}^{Born} = \mathcal{M}_{++TL}^{Born} = \mathcal{M}_{+++-}^{Born} = \mathcal{M}_{++-+}^{Born} = 0. \tag{2.13}$$

It follows that corresponding one-loop amplitudes, which are not zero, do not contribute to the interference term if the cross section is integrated over the phase space of the W 's decay products. However, they do contribute if angular distributions and correlations of the decay products are reconstructed.

3. Born Cross Sections

The lowest order polarized cross sections at high energy $s \gg M_W^2$ are given by (see also the full Born helicity amplitudes and cross sections [8, 9, 12])

$$\begin{aligned}
\int_{p_T^W > p_T} d\sigma_{++++}^{Born} &= \frac{8\pi\alpha^2}{p_T^2} + \dots \xrightarrow{p_T \rightarrow 0} \frac{8\pi\alpha^2}{M_W^2} \\
\int_{p_T^W > p_T} d\sigma_{++00}^{Born} &= \frac{8\pi\alpha^2 M_W^4}{p_T^2 s^2} + \dots \xrightarrow{p_T \rightarrow 0} \frac{8\pi\alpha^2 M_W^2}{s^2}
\end{aligned}$$

$$\begin{aligned}
\int_{p_T^W > p_T} d\sigma_{++--}^{Born} &= \frac{8\pi\alpha^2 M_W^8}{p_T^2 s^4} + \dots \xrightarrow[p_T \rightarrow 0]{} \frac{8\pi\alpha^2 M_W^6}{s^4} \\
\int_{p_T^W > p_T} d\sigma_{+-+-+}^{Born} &= \frac{4\pi\alpha^2}{p_T^2} + \dots \xrightarrow[p_T \rightarrow 0]{} \frac{4\pi\alpha^2}{M_W^2} \\
\int_{p_T^W > p_T} d\sigma_{+-00}^{Born} &= \frac{4\pi\alpha^2}{s} + \dots \\
\int_{p_T^W > p_T} d\sigma_{+-+0}^{Born} &= \frac{32\pi\alpha^2 M_W^2}{s^2} \left(\ln \frac{s}{p_T^2} - 1 \right) + \dots \xrightarrow[p_T \rightarrow 0]{} \frac{32\pi\alpha^2 M_W^2}{s^2} \left(\ln \frac{s}{M_W^2} - 2 \right) \\
\int_{p_T^W > p_T} d\sigma_{+-+-+}^{Born} &= \frac{64\pi\alpha^2 M_W^4}{s^3} + \dots
\end{aligned} \tag{3.1}$$

The first column shows the cross sections integrated over a region $p_T^W > p_T$, for $s \gg p_T^2 \gg M_W^2$. The last column shows the cross sections integrated over the whole phase space. For initial helicities $+00$ and $+++$ these two limit coincide. As is well known (see *e.g.* [28]), the asymptotic behavior of the scattering amplitudes is determined by the exchange of the spin-one particle in the t -channel and in the Born approximation is given by

$$\mathcal{M}_{\lambda_1\lambda_2\lambda_3\lambda_4} \Bigg|_{\substack{s \rightarrow \infty \\ t \sim M_W^2}} \propto \frac{2s}{t - M_W^2} \delta_{\lambda_1\lambda_4} \delta_{\lambda_2\lambda_3}, \tag{3.2}$$

so that the cross sections integrated over the whole phase space are non-decreasing with energy for helicity conserving amplitudes. Asymptotically

$$\sigma_{+-+-}^{Born} = \sigma_{+-+-+}^{Born} = \frac{1}{2} \sigma_{+++-}^{Born}, \tag{3.3}$$

and total cross sections of WW -pair production are the same for $++$ and $+-$ initial photon helicities.

As initial photons are necessarily transversely polarized, cross section of transverse $W_T W_T$ pair production dominates. For a finite angular cut even the dominating cross sections do decrease as $1/s$, but still they are much larger than the suppressed cross sections because they are still enhanced by a large factor of s/p_T^2 . A cross section σ_{+-00} is the next to the largest ones σ_{+++-} , σ_{+-+-+} and it is decreasing as $1/s$. The other cross sections decrease for finite angular cuts as $1/s^2$ (σ_{+-+0}), $1/s^3$ (σ_{++00} , σ_{+-+-+}), and even as $1/s^5$ (σ_{+-+-}). The cross sections σ_{++LT} and σ_{+++-} vanish at the Born level.

4. $\mathcal{O}(\alpha)$ corrections

Inclusive cross section of W^+W^- pair production in photon-photon collisions to third order in α is given by the sum of Born cross section, interference term between the Born and one-loop amplitudes and cross section of W^+W^- pair production accompanied by the real photon emission. At energies above the WWZ threshold one should add the cross section of W^+W^-Z production. In principle one can also add the cross section of associated Higgs boson production $\gamma\gamma \rightarrow W^+W^-H$. It seems

however unreasonable to consider here associated Higgs production on an equal footing with gauge boson production, as it definitely deserves a special consideration [13, 19]. Anyway, since the cross section of W^+W^-H production is at least an order of magnitude smaller than that of W^+W^-Z , its contribution to corrections to $\gamma\gamma \rightarrow W^+W^-$ cross section can be safely neglected. Since one-loop amplitude and soft photon emission cross section are IR-divergent and only their sum is IR-finite it is convenient, as usual, to consider soft and hard photon emission separately. Finally, the inclusive cross section of W^+W^- pair production in photon-photon collisions can be represented as a sum

$$\begin{aligned} d\sigma(\gamma\gamma \rightarrow W^+W^- + X) &= \quad (4.1) \\ d\sigma^{Born}(\gamma\gamma \rightarrow W^+W^-) &+ \frac{1}{2s_{\gamma\gamma}} 2 \operatorname{Re} \left(\mathcal{M}^{Born} \mathcal{M}^{1-loop*} \right) dPS^{(2)} \\ &+ d\sigma^{soft}(\gamma\gamma \rightarrow W^+W^-\gamma) \Big|_{\omega_\gamma < k_c} + d\sigma^{hard}(\gamma\gamma \rightarrow W^+W^-\gamma) \Big|_{\omega_\gamma > k_c} + d\sigma^Z(\gamma\gamma \rightarrow W^+W^-Z). \end{aligned}$$

Analytical expression in terms of Spence functions for the IR-divergent factorizable soft photon emission cross section is given by

$$d\sigma^{soft}(\gamma\gamma \rightarrow W^+W^-\gamma) = d\sigma^{Born}(\gamma\gamma \rightarrow W^+W^-) R^{soft}, \quad (4.2)$$

where

$$\begin{aligned} R^{soft} &= \frac{2\alpha}{\pi} \left\{ \left(-1 + \frac{1}{\beta} \left(1 - \frac{2M_W^2}{s} \right) \ln \left(\frac{1+\beta}{1-\beta} \right) \right) \ln \left(\frac{2k_c}{\lambda} \right) \right. \\ &\quad \left. + \frac{1}{2\beta} \ln \left(\frac{1+\beta}{1-\beta} \right) + \frac{1}{2\beta} \left(1 - \frac{2M_W^2}{s} \right) \left[Sp \left(\frac{-2\beta}{1-\beta} \right) - Sp \left(\frac{2\beta}{1+\beta} \right) \right] \right\} \end{aligned} \quad (4.3)$$

and λ is fictitious photon mass, k_c is the soft photon energy cutoff and $\beta = \sqrt{1 - 4M_W^2/s}$.

The cross section of hard photon emission is given by

$$\sigma_{\lambda_1\lambda_2\lambda_3\lambda_4}^{hard}(\gamma\gamma \rightarrow W^+W^-\gamma) = \frac{1}{2s_{\gamma\gamma}} \int \sum_{\lambda_5} |\mathcal{M}_{\lambda_1\lambda_2\lambda_3\lambda_4\lambda_5}(\gamma\gamma \rightarrow W^+W^-\gamma)|^2 dPS^{(3)}, \quad (4.4)$$

where the three particle phase space can be represented in the following form

$$dPS^{(3)} = \frac{1}{4(2\pi)^3} \omega_\gamma^2 \beta_{+-} d\ln \omega_\gamma d\cos \chi d\cos \theta^+ d\cos \theta^-. \quad (4.5)$$

Here ω_γ is the final photon energy in c.m.s. of colliding initial photons, χ is the final photon – W angle in the c.m.s. of W^+W^- system, θ^\pm are the initial photon – W^\pm angles in c.m.s. of colliding photons and $\beta_{+-} = \sqrt{1 - 4M_W^2/s_{W^+W^-}}$. The cross section of W^+W^-Z production is given by the analogous formulas.

Total $\mathcal{O}(\alpha)$ correction is defined by

$$\sigma(\gamma\gamma \rightarrow W^+W^- + X) = \sigma^{Born}(\gamma\gamma \rightarrow W^+W^-) (1 + \delta^{tot}). \quad (4.6)$$

According to (4.1) it can be decomposed as

$$\delta^{tot} = \delta^{virt} + \delta^{soft} + \delta^{hard} + \delta^Z. \quad (4.7)$$

On-shell renormalization scheme [20] and 't Hooft-Feynman gauge are used to calculate loop corrections, *i.e.* fine-structure constant α and the physical particle masses are used as basic parameters. The width of the Higgs boson resonance is included in a gauge invariant manner, as described *e.g.* in Ref. [21].

The calculation has been performed using symbolic manipulation program *FORM* [22] to generate Feynman diagrams and to reduce tensor loop integrals to scalar one-loop one-, two-, three- and four-point functions A , B , C and D [23, 24]. *FF*-package [25] has been used for the numeric evaluation of the scalar loop integrals. The $\gamma\gamma \rightarrow W^+W^-\gamma$, W^+W^-Z helicity amplitudes have also been evaluated with *FORM*. For the phase space integration we have used the multi-dimensional Monte Carlo integration package *BASES* [26].

5. The structure of leading corrections

As it was already mentioned in the literature [6, 7, 18], no power or logarithmically enhanced corrections involving m_H^2/M_W^2 , $\log(m_H^2)$, m_t^2/M_W^2 or $\log(m_t^2)$ appear in the on-shell scheme in the limit, when Higgs-boson or top-quark masses are much larger than the collision energy. The explanation of this fact is given by the low energy theorem, according to which the cross section of the Compton scattering of the photon off the W -boson target, when photon energy tends to zero, to all orders is given by the Born cross section with the universally renormalized on-shell electric charge [20]

$$e^R = \left(Z_{AA}^{1/2} - \frac{s_W^0}{c_W^0} Z_{ZA}^{1/2} \right) e^0. \quad (5.1)$$

Here the charge universality means that electric charge measured in the photon scattering off W -boson is equal to the charge measured in photon-electron Compton scattering. Since large masses m_H , m_t can be considered as gauge invariant cutoffs, divergent in the limit $m_H^2, m_t^2 \gg s, -t, -u$ contributions should take a form of local gauge invariant three- and four-vertex corrections, *i.e.* their contribution to the amplitude of the Compton photon- W scattering should be proportional to the Born amplitude. Moreover, this contribution should be canceled after the counterterms are taken into account in order to guarantee the charge universality.

Indeed, if we include only the tadpole and W -boson mass counterterms, to fix a mass of the W -boson, the divergent in the heavy mass limit amplitudes are given by

$$\mathcal{M}_{div}^{bose} = -\frac{\alpha}{48\pi s_W^2} \log(m_H^2) \mathcal{M}^{Born}, \quad (5.2)$$

$$\mathcal{M}_{div}^{fermi} = -\frac{\alpha N_c}{12\pi s_W^2} \log(m_t^2) \mathcal{M}^{Born}. \quad (5.3)$$

As soon as the W -boson wave function renormalization constant is taken into account these divergent contributions are really canceled out (renormalization constants $Z_{AA}^{1/2}$, $Z_{ZA}^{1/2}$ contain no logs or positive powers of the ratios m_H^2/M_W^2 , m_t^2/M_W^2 at one-loop level).

Instead of rising with m_H , m_t corrections, rising with energy contributions still remain [5, 7] as a result of violation of unitarity cancellations in this limit. Namely, in the limit $M_W^2 \ll s, -t, -u \ll m_H^2$ the following helicity amplitudes exhibit rising contributions

$$\mathcal{M}_{++00}^{bose} = \frac{5\alpha^2}{12s_W^2} \frac{s}{M_W^2}, \quad (5.4)$$

$$\mathcal{M}_{+++0}^{bose} = \frac{\alpha^2}{6\sqrt{2}s_W^2} \frac{t-u}{M_W p_T}, \quad (5.5)$$

$$\mathcal{M}_{+-+0}^{bose} = -\frac{\alpha^2}{6\sqrt{2}s_W^2} \frac{t}{M_W p_T}. \quad (5.6)$$

The heavy top-quark contributions in the limit $M_W^2 \ll s, -t, -u \ll m_t^2$ are given by

$$\mathcal{M}_{+++\pm}^{fermi} = \mathcal{M}_{++-\pm}^{fermi} = -\frac{4\alpha^2 N_c}{27s_W^2} \frac{s}{s-m_H^2}, \quad (5.7)$$

$$\mathcal{M}_{++00}^{fermi} = -\frac{\alpha^2 N_c}{54s_W^2} \frac{s}{M_W^2} - \frac{4\alpha^2 N_c}{27s_W^2} \frac{s}{s-m_H^2} \left(\frac{m_H^2}{2M_W^2} - 1 \right), \quad (5.8)$$

$$\mathcal{M}_{+-+0}^{fermi} = \frac{\alpha^2 N_c}{6\sqrt{2}s_W^2} \frac{s-t}{s} \frac{t}{M_W p_T}. \quad (5.9)$$

In addition, at energies much larger than m_H , m_t power corrections proportional to m_H^2/M_W^2 , m_t^2/M_W^2 do appear as a consequence of incomplete unitarity cancellations. For $M_W^2 \ll m_H^2 \ll s, -t, -u$ we have²

$$\mathcal{M}_{++00}^{bose} = -\frac{\alpha^2}{s_W^2} \frac{m_H^2}{M_W^2}, \quad (5.10)$$

$$\mathcal{M}_{+-00}^{bose} = \frac{\alpha^2}{4s_W^2} \frac{m_H^2}{M_W^2}. \quad (5.11)$$

The leading top-quark contributions in the limit $M_W^2 \ll m_t^2 \ll s, -t, -u$ are given by

$$\mathcal{M}_{+++\pm}^{fermi} = \mathcal{M}_{++-\pm}^{fermi} = \frac{16\alpha^2 N_c}{9s_W^2} \frac{m_t^2}{s-m_H^2}, \quad (5.12)$$

$$\mathcal{M}_{++00}^{fermi} = \frac{5\alpha^2 N_c}{9s_W^2} \frac{m_t^2}{M_W^2} + \frac{16\alpha^2 N_c}{9s_W^2} \frac{m_t^2}{s-m_H^2} \left(\frac{m_H^2}{2M_W^2} - 1 \right), \quad (5.13)$$

$$\mathcal{M}_{+-00}^{fermi} = \frac{\alpha^2 N_c}{s_W^2} \frac{m_t^2}{M_W^2} \left\{ \frac{5}{18} \frac{t}{u} \left(\log^2 \left(\frac{s}{t} - i\epsilon \right) + \pi^2 \right) + \log \left(-\frac{t}{m_t^2} \right) - \frac{3}{2} \right\}. \quad (5.14)$$

Cross sections of the longitudinal $W_L W_L$ pair production are the most sensitive to the mechanism of the electroweak symmetry breaking. Although the dependence is quite strong $\propto m_H^2, m_t^2$ (5.10)–(5.14), the cross sections $\sigma_{+\pm 00}$ themselves are quite small in comparison to cross section of transverse $W_T W_T$ pair production and it will be very difficult to measure Higgs or top quark couplings with longitudinal weak bosons in this reaction.

Another very important feature of radiative corrections to $\gamma\gamma \rightarrow W^+W^-$, also mentioned in the Refs. [18], is that no large logarithms containing light fermion masses $\log(s/m_f^2)$ remain in the renormalized amplitude, so that not running $\alpha \approx 1/129$ at $q^2 = M_W^2$, but fine-structure constant $\alpha = 1/137.036$ at zero momentum is relevant for this reaction. For γW Compton scattering near the threshold this property is an immediate consequence of the low energy theorem and charge universality mentioned above and it should be true to any order of α . In fact, at one-loop level one can easily show, that these large logarithms cancel at any energy. More specifically, mass singularities coming from the light fermion contributions to the scalar loop integrals are canceled

²The right hand side of equation (11) of Ref. [7] should be multiplied by 2.

out in the total unrenormalized amplitude as a consequence of the Kinoshita-Lee-Nauenberg (KLN) theorem [27]. Due to the identity (5.1), singular terms that are present in the photon wave function renormalization constant $Z_{AA}^{1/2}$ are canceled by the corresponding terms in the renormalization constant of the electric charge. The fermion contribution to constant $Z_{ZA}^{1/2}$ is equal to zero at one-loop level.

And last but not least, the asymptotic behavior of the dominating gauge vector boson scattering amplitude in the leading logarithmic approximation at high energy and fixed momentum transfers $s \gg -t, M_W^2$, related to the exchange of spin-one and isospin $I = 1$ particle in the t -channel, is known (see, *e.g.* [28, 29]) to have the Regge form

$$\mathcal{M}_{\lambda_1 \lambda_2 \lambda_3 \lambda_4}(s, t, u) \Big|_{I=1} \propto \frac{g^2}{t - M_W^2} \delta_{\lambda_1 \lambda_4} \delta_{\lambda_2 \lambda_3} \left((-s)^{1+\alpha(t)} - (-u)^{1+\alpha(t)} \right). \quad (5.15)$$

Here the trajectory $\alpha(t)$ is given by

$$\alpha(q^2) = \frac{g^2}{(2\pi)^3} (q^2 - M_W^2) \int \frac{d^2 k_\perp}{(k_\perp^2 - M_W^2) ((k_\perp + q)^2 - M_W^2)}, \quad (5.16)$$

$$\alpha(0) = -\frac{g^2}{8\pi^2}, \quad \alpha(t) \Big|_{-t \gg M_W^2} \sim -\frac{g^2}{4\pi^2} \log(-t/M_W^2). \quad (5.17)$$

In fact, the equation (5.15) was explicitly checked up to the eights order of perturbation theory for the gauge group $SU(2)$ [28, 29].

With the help of the equations (5.15)–(5.17) one can easily derive, that total $\mathcal{O}(\alpha)$ bosonic one-loop correction to the total cross section of vector boson scattering, including virtual corrections as well as real triple vector boson production grows as $\log(s/M_W^2)$ and is given by

$$\delta^{tot} = \frac{\text{Im } \mathcal{M}^{2-loop}}{\text{Im } \mathcal{M}^{1-loop}} \Big|_{t=0} = \alpha(0) \log(s/M_W^2) = -\frac{\alpha}{2\pi s_W^2} \log(s/M_W^2). \quad (5.18)$$

So, one can guess that electroweak corrections to the total $\gamma\gamma \rightarrow W^+W^-$ cross section are negative (because the trajectory $\alpha(t)$ (5.16) is negative) and range from $\sim -1\%$ at $\sqrt{s} = 300$ GeV to $\sim -3\%$ at $\sqrt{s} = 1$ TeV.

From the other side, one can estimate the value of radiative corrections in the central region of W^+W^- production by just integrating the one-loop scattering cross section (5.15) in this region

$$\delta^{virt}(|t| > |t_0|) \approx -2 \frac{\alpha}{\pi s_W^2} \log(s/M_W^2) \log(-t_0/M_W^2). \quad (5.19)$$

So, one should expect that corrections to $\gamma\gamma \rightarrow W^+W^-$ cross section in the central region grow as $\log^2(s/M_W^2)$ and could be 5 \div 10 times larger than corrections to the total cross section at TeV energies.

6. Numerical results

The following set of parameters was used [30]

$$\begin{aligned} \alpha &= 1/137.0359895 \\ M_Z &= 91.187 \text{ GeV}, & M_W &= 80.36 \text{ GeV}, & m_H &= 300 \text{ GeV} \\ m_e &= 0.51099907 \text{ MeV}, & m_u &= 48 \text{ MeV}, & m_d &= m_u, \\ m_\mu &= 0.105658389 \text{ GeV}, & m_c &= 1.5 \text{ GeV}, & m_s &= 150 \text{ MeV}, \\ m_\tau &= 1.777 \text{ GeV}, & m_t &= 180 \text{ GeV}, & m_b &= 4.5 \text{ GeV}. \end{aligned}$$

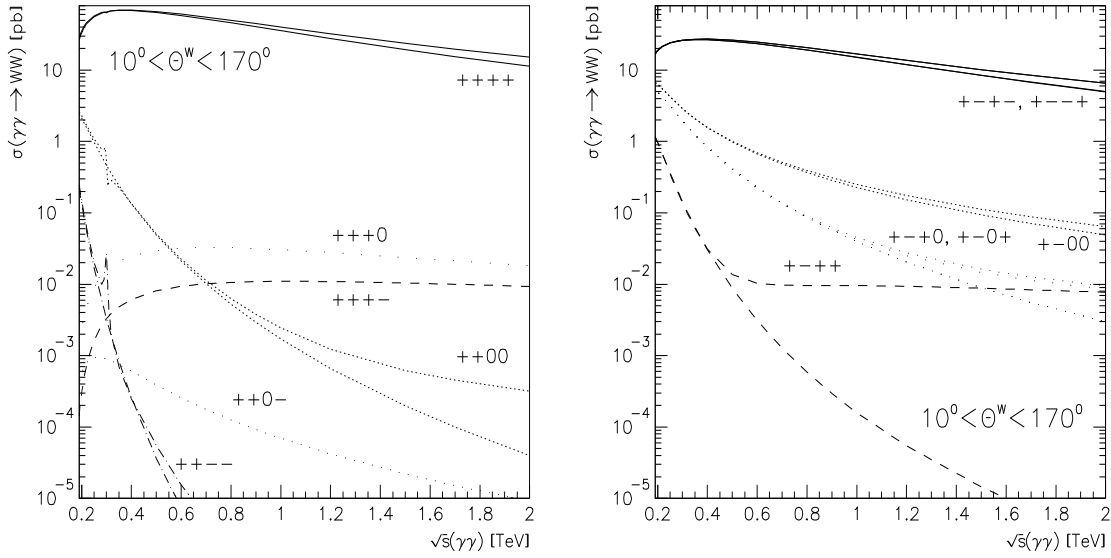


Fig. 1. Total cross sections of $WW(\gamma)$ production for various polarizations. Born and corrected cross sections are shown. The curves nearest to the helicity notations represent the corrected cross sections.

The unit Cabibbo-Kobayashi-Maskawa matrix was used and the W -boson width was neglected.

An important issue relates to the choice of the photon spectrum at $\gamma\gamma$ collider. In principle, it is possible to adjust the parameters of the laser to obtain a spectrum most suitable for gauge boson production, one that is polarized and peaked at high energies [1]. However, the precise high energy photon spectrum depends on the beam polarization, conversion distance and other technical parameters [1–3] and can vary from one scheme to the other and the shape of the predicted ideal spectrum [1] can be severely distorted [2, 3]. Since the detailed studies and choices of the optimal parameters have not been made yet, we prefer to present our results for the case of monochromatic photon spectrum. As a worst case scenario, the effect of non-monochromaticity can be estimated with a luminosity in the peak that is ten times smaller than the total photon-photon luminosity.

Since photon energy distribution in the reaction of $W^+W^-\gamma$ production strongly peaks at low energies it will not be easy to experimentally separate W^+W^- pair production from $W^+W^-\gamma$ production. Moreover, in realistic case the energy of the initial photons will not be fixed because of the quite wide spectrum of the Compton backscattered photons [1–3], and it will not be possible to require that W -bosons would be produced back-to-back to suppress real photon emission. So, in what follows we just integrate over the whole photon phase space available. Angular cuts will be imposed only on W^\pm production angles.

Figure 1 shows total cross section of WW pair production summed over WW and $WW\gamma$ final states and integrated over W^\pm scattering angles in the interval $10^\circ < \theta^\pm < 170^\circ$ as a function of energy for various polarizations. As we have discussed in Sections 3, 5 the bulk of the cross section originates from transverse W_TW_T pair production. Transverse W 's are produced predominantly in the forward/backward direction and the helicity conserving amplitudes are dominating. Cross sections integrated over the whole phase space are non-decreasing with energy. For a finite angular

Table 1. Total Born cross sections and relative corrections for various polarizations. When Born cross section is equal to zero cross sections of hard photon emission are given instead of relative corrections. The W^\pm production angle is restricted to $10^\circ < \theta^\pm < 170^\circ$. WWZ production is not included.

$\sqrt{s} = 500 \text{ GeV}$						
$\lambda_1\lambda_2\lambda_3\lambda_4$	σ^{Born}, pb	$\delta^{hard}, \%$	$\delta^{soft}, \%$	$\delta^{bose}, \%$	$\delta^{fermi}, \%$	$\delta^{tot}, \%$
unpol	60.71	7.89	2.30	-13.0	-0.242	-3.06
$++TT$	66.12	7.91	2.30	-13.0	-0.137	-2.93
$++TL$	0	$6.01 \cdot 10^{-2} \text{ pb}$	0	0	0	-
$++LL$	$4.913 \cdot 10^{-2}$	13.7	2.30	-22.4	9.89	3.78
$+-TT$	52.58	7.66	2.30	-13.0	-0.309	-3.37
$+-TL$	1.669	10.2	2.30	-12.6	-3.06	-3.18
$+-LL$	0.9989	8.20	2.30	-12.6	0.575	-1.53

$\sqrt{s} = 1000 \text{ GeV}$						
$\lambda_1\lambda_2\lambda_3\lambda_4$	σ^{Born}, pb	$\delta^{hard}, \%$	$\delta^{soft}, \%$	$\delta^{bose}, \%$	$\delta^{fermi}, \%$	$\delta^{tot}, \%$
unpol	37.04	13.4	3.11	-25.7	-1.28	-10.5
$++TT$	40.08	13.4	3.11	-26.4	-1.30	-11.1
$++TL$	0	$6.13 \cdot 10^{-2} \text{ pb}$	0	0	0	-
$++LL$	$1.715 \cdot 10^{-3}$	64.3	3.11	-34.8	10.3	42.9
$+-TT$	33.60	13.1	3.11	-25.0	-1.19	-10.0
$+-TL$	0.1577	40.5	3.11	-21.9	-10.6	11.2
$+-LL$	0.2510	14.2	3.11	-24.4	-2.82	-9.86

$\sqrt{s} = 2000 \text{ GeV}$						
$\lambda_1\lambda_2\lambda_3\lambda_4$	σ^{Born}, pb	$\delta^{hard}, \%$	$\delta^{soft}, \%$	$\delta^{bose}, \%$	$\delta^{fermi}, \%$	$\delta^{tot}, \%$
unpol	14.14	20.1	3.49	-45.1	-2.99	-24.5
$++TT$	15.17	20.0	3.49	-46.1	-3.03	-25.6
$++TL$	0	$3.65 \cdot 10^{-2} \text{ pb}$	0	0	0	-
$++LL$	$3.979 \cdot 10^{-5}$	749.	3.49	-84.8	35.0	702.
$+-TT$	13.04	19.6	3.49	-44.0	-2.89	-23.8
$+-TL$	$1.197 \cdot 10^{-2}$	248.	3.49	-29.8	-22.2	199.
$+-LL$	$6.364 \cdot 10^{-2}$	21.0	3.49	-40.2	-7.75	-23.4

cutoff they do decrease as $1/s$, but still they are much larger than suppressed cross sections. For the dominating $+++$, $+-+$, $+-+$ helicity configurations corrections are negative and they rise with energy ranging from -3% at 500 GeV to -25% at 2 TeV. The correction for the next to the largest cross section σ_{+-00} is also negative. For the other helicities radiative corrections are positive at high energies due to dominating positive contribution of real photon emission. Radiative corrections to cross sections σ_{+-TL} , which are decreasing at Born level as $1/s^2$, are positive and large. For the cross sections σ_{++00} and σ_{+++-} , which are decreasing as $1/s^3$ for a finite angular cutoff, corrections are even larger. The cross section σ_{++--} is decreasing at tree level as $1/s^5$ for a finite angular cutoff and is quite negligible at high energy. The cross sections σ_{++LT} and σ_{+++-} vanish at the Born level, so only the process of $WW\gamma$ production contributes in Figure 1. The cross sections σ_{++--} and σ_{++00} exhibit a clear Higgs resonance peak and the interference pattern, respectively. The dominating σ_{++++} cross section has a hardly visible in logarithmic scale dip at $\sqrt{s_{\gamma\gamma}} = m_H = 300$ GeV [8]. A very high WW mass resolution and high luminosity will be required to register such a dip experimentally.

Table 1 presents Born cross sections and relative corrections for various polarizations and energies. Total corrections, corrections originating from virtual bosonic and fermionic contributions $\delta^{virt} = \delta^{bose} + \delta^{fermi}$ as well as from soft and hard photon emission are shown separately. Fictitious photon mass $\lambda = 10^{-2}$ GeV is used to regularize infrared divergences and a photon energy cutoff $k_c = 0.1$ GeV discriminates between soft and hard bremsstrahlung. Looking at the Table 1 one concludes that bosonic corrections are obviously dominating over fermionic ones.

Figures 2-4 show the values of the cross sections and $\mathcal{O}(\alpha)$ relative corrections for the WW -pair production in the central region for various helicities at $\sqrt{s_{\gamma\gamma}} = 0.5, 1$ and 2 TeV. As expected, corrections for the dominating transverse $W_T W_T$ -pair production are several times larger in the central region. As the Born cross section σ_{++++} of $W^+ W^-$ production at $\theta_W = 90^\circ$ is asymptotically 16 times larger than σ_{++-+} , σ_{+-++} , curves for the cross sections σ_{++-+} , σ_{+-++} fall more rapidly than σ_{++++} and at $\theta_W = 60 \div 70^\circ$ the subdominant σ_{+-00} is equal to the dominant one. The cross sections for all the other helicities are at least an order of magnitude smaller than the dominant ones in the whole region of $\cos \theta_W$.

In Table 2 Born cross sections and relative corrections are given for several intervals of W^\pm scattering angles. At high energies large cancellations occur between negative virtual corrections and positive corrections corresponding to real photon or Z -boson emission, as one should expect, as at high energies, $s \gg M_W^2$, collinear singularities should cancel out only in the sum of virtual, soft and hard contributions again as a consequence of KLN theorem. Consequently, although the correction originating from the WWZ production is completely negligible at $\sqrt{s_{\gamma\gamma}} = 0.3$ TeV, it is of the same order of magnitude as hard photon correction at 2 TeV. The size of the total corrections is in rough agreement with the values expected on the basis of leading logarithmic corrections discussed at the end of the Section 5. Corrections in the central region $60^\circ < \theta < 120^\circ$ are really $5 \div 8$ times larger than the corrections to the total cross section at $0.5 \div 2$ TeV.

Although the fermionic one-loop corrections are small, only they give nonvanishing contribution to P - or C -violating asymmetries. As an example of such a quantity we consider the P -odd forward-backward asymmetry

$$A_{\lambda_3 \lambda_4}^{FB} = \frac{\sigma_{+-\lambda_3 \lambda_4}(\cos \theta^{W^+} > 0) - \sigma_{+-(-\lambda_3)(-\lambda_4)}(\cos \theta^{W^+} < 0)}{\sigma_{+-\lambda_3 \lambda_4}(\cos \theta^{W^+} > 0) + \sigma_{+-(-\lambda_3)(-\lambda_4)}(\cos \theta^{W^+} < 0)} \quad (6.1)$$

Figure 5 presents the forward-backward asymmetry for various helicities as a function of c.m.s. energy. For the dominant transverse σ_{++-+} , σ_{+-++} cross sections the asymmetry at high energy is negative and less than 0.5%. Even for the subdominant σ_{+-00} cross section the asymmetry is

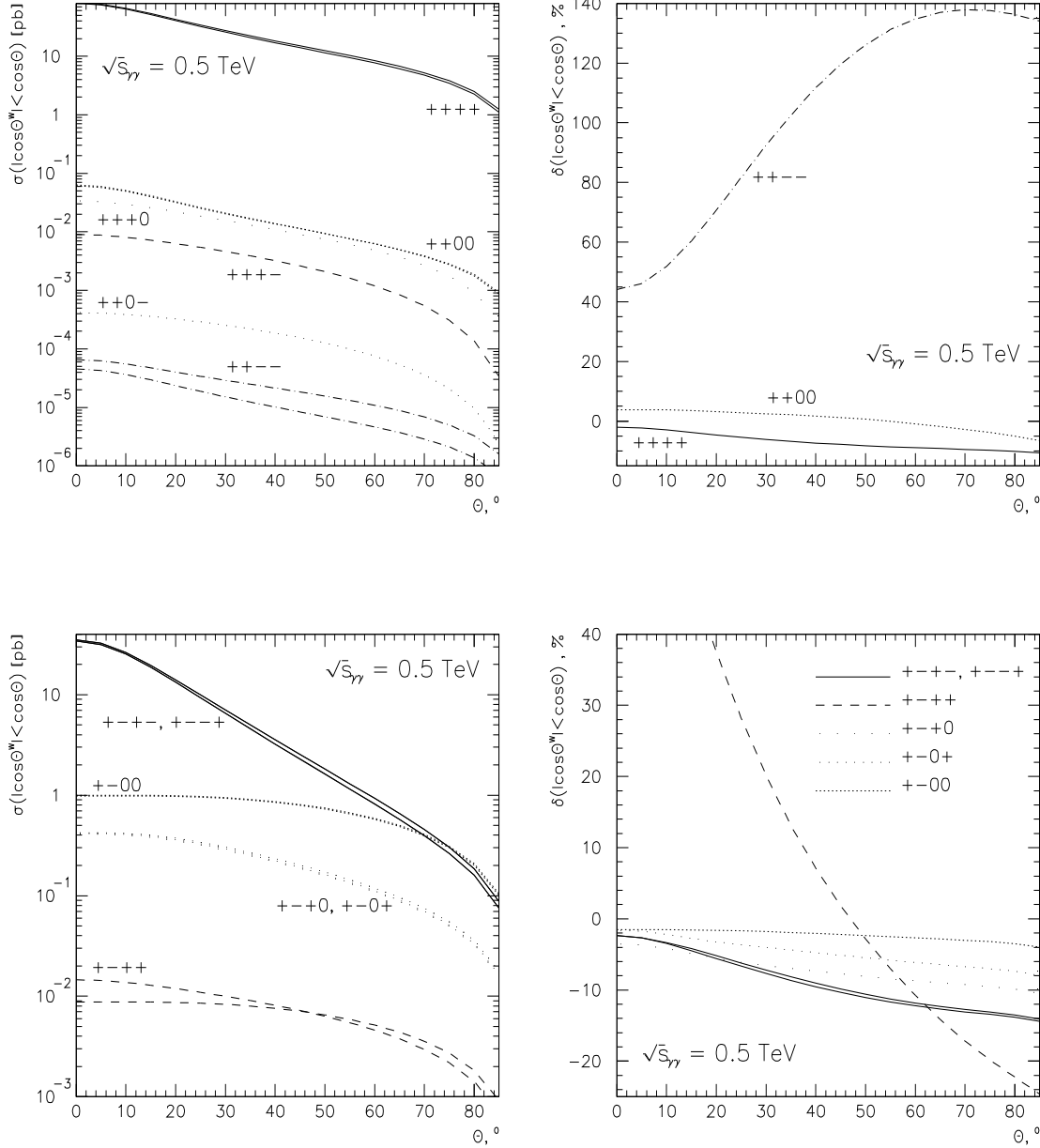


Fig. 2. Cross sections and relative corrections for $W^+W^-(\gamma)$ production in the region $|\cos\theta^\pm| < \cos\theta$ for various polarizations as a function of $\cos\theta$ at $\sqrt{s_{\gamma\gamma}} = 0.5$ TeV. Born and corrected cross sections are shown. The curves nearest to the helicity notations represent the corrected cross sections.

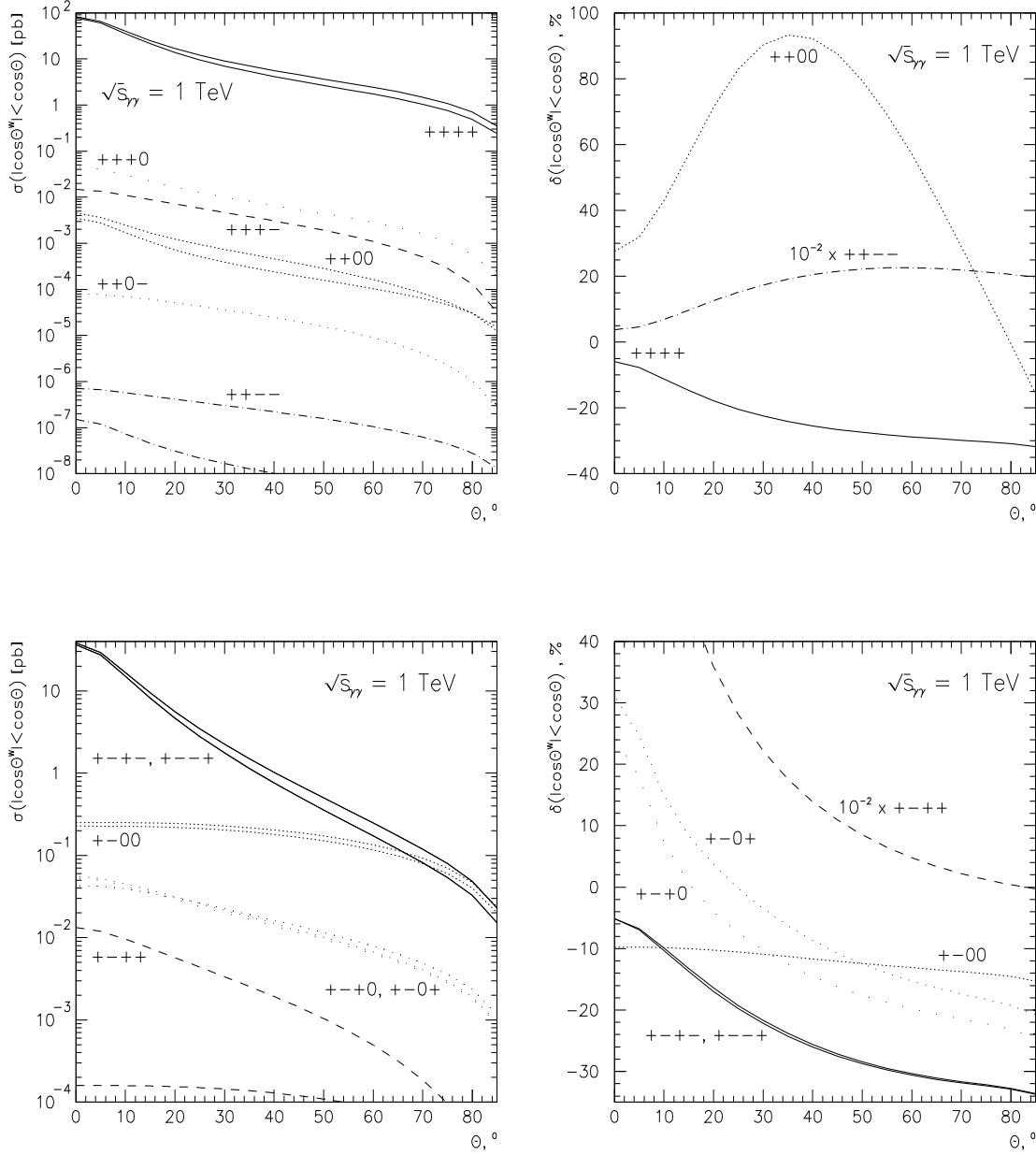


Fig. 3. The same as Fig. 2 at $\sqrt{s_{\gamma\gamma}} = 1$ TeV. Since relative corrections to suppressed at high energy Born cross sections σ_{++--} , σ_{+-+-} are quite large, corresponding curves are shown multiplied by a factor of 10^{-2} .

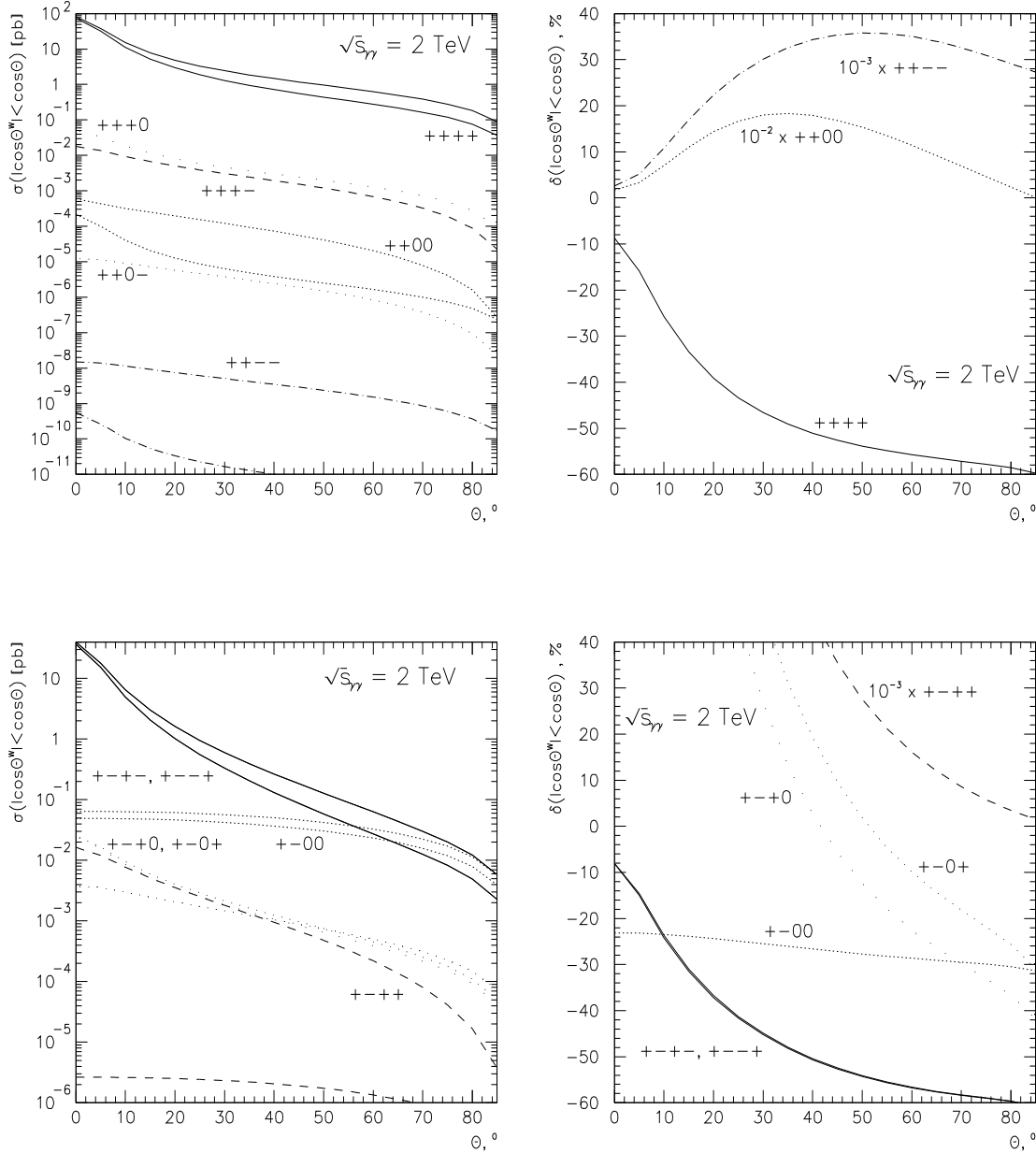


Fig. 4. The same as Fig. 2 at $\sqrt{s_{\gamma\gamma}} = 2$ TeV. Relative corrections are shown rescaled by a factor of 10^{-3} for the cross sections σ_{++--} , σ_{+-+-} and by a factor of 10^{-2} for σ_{++00} .

Table 2. Total unpolarized Born cross sections and relative corrections for various intervals of W^\pm scattering angles. Corrections originating from real hard photon ($\omega_\gamma > k_c = 0.1$ GeV) and Z -boson emission as well as IR-finite sum of soft photon and virtual boson contributions, fermion virtual corrections and total corrections are given separately.

$\sqrt{s} = 300$ GeV						
$\theta_{W^\pm}, {}^\circ$	σ^{Born}, pb	$\delta^{hard}, \%$	$\delta^Z, \%$	$\delta^{soft+bose}, \%$	$\delta^{fermi}, \%$	$\delta^{tot}, \%$
$0^\circ < \theta < 180^\circ$	70.22	4.15	$2.64 \cdot 10^{-2}$	-7.09	0.327	-1.37
$10^\circ < \theta < 170^\circ$	64.46	4.11	$2.74 \cdot 10^{-2}$	-7.31	0.257	-1.59
$30^\circ < \theta < 150^\circ$	38.15	4.09	$3.27 \cdot 10^{-2}$	-8.62	-0.123	-2.67
$60^\circ < \theta < 120^\circ$	12.96	4.02	$2.94 \cdot 10^{-2}$	-10.7	-0.415	-3.75

$\sqrt{s} = 500$ GeV

$\theta_{W^\pm}, {}^\circ$	σ^{Born}, pb	$\delta^{hard}, \%$	$\delta^Z, \%$	$\delta^{soft+bose}, \%$	$\delta^{fermi}, \%$	$\delta^{tot}, \%$
$0^\circ < \theta < 180^\circ$	77.50	7.96	0.468	-10.1	$9.04 \cdot 10^{-2}$	-1.63
$10^\circ < \theta < 170^\circ$	60.71	7.89	0.541	-10.7	-0.242	-2.52
$30^\circ < \theta < 150^\circ$	21.85	8.05	0.817	-13.0	-1.34	-5.50
$60^\circ < \theta < 120^\circ$	5.681	8.02	0.789	-14.8	-2.13	-8.12

$\sqrt{s} = 1000$ GeV

$\theta_{W^\pm}, {}^\circ$	σ^{Born}, pb	$\delta^{hard}, \%$	$\delta^Z, \%$	$\delta^{soft+bose}, \%$	$\delta^{fermi}, \%$	$\delta^{tot}, \%$
$0^\circ < \theta < 180^\circ$	79.99	13.3	1.55	-18.7	$-5.51 \cdot 10^{-2}$	-3.89
$10^\circ < \theta < 170^\circ$	37.04	13.4	2.39	-22.6	-1.28	-8.10
$30^\circ < \theta < 150^\circ$	6.924	14.2	3.96	-32.1	-3.80	-17.8
$60^\circ < \theta < 120^\circ$	1.542	14.2	3.88	-37.1	-5.13	-24.1

$\sqrt{s} = 2000$ GeV

$\theta_{W^\pm}, {}^\circ$	σ^{Born}, pb	$\delta^{hard}, \%$	$\delta^Z, \%$	$\delta^{soft+bose}, \%$	$\delta^{fermi}, \%$	$\delta^{tot}, \%$
$0^\circ < \theta < 180^\circ$	80.53	19.0	2.91	-27.2	$-7.45 \cdot 10^{-2}$	-5.33
$10^\circ < \theta < 170^\circ$	14.14	20.1	6.38	-41.6	-2.99	-18.1
$30^\circ < \theta < 150^\circ$	1.848	21.5	9.77	-60.1	-6.54	-35.4
$60^\circ < \theta < 120^\circ$	0.3936	21.6	9.60	-67.6	-8.04	-44.5

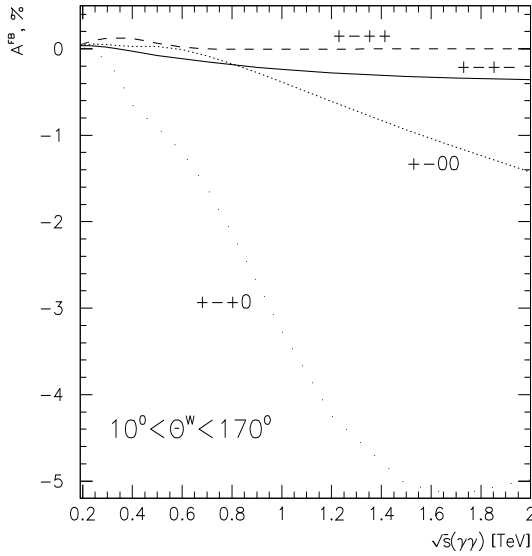


Fig. 5. P -odd forward-backward asymmetry as a function of the center-of-mass energy.

negative and smaller than 1.5% up to 2 TeV. For the suppressed cross sections σ_{+-+0} , σ_{+--0} the fermionic contribution gives rise to the asymmetry of about -5% at high energy.

Another example of the asymmetry, that could be used for the measurement of the W -boson anomalous magnetic and quadrupole moments[31] is given by the so called polarization asymmetry

$$A^{+-} = \frac{\sum_{\lambda_i} (\sigma_{++\lambda_3\lambda_4(\lambda_5)} - \sigma_{+-\lambda_3\lambda_4(\lambda_5)})}{\sum_{\lambda_i} (\sigma_{++\lambda_3\lambda_4(\lambda_5)} + \sigma_{+-\lambda_3\lambda_4(\lambda_5)})}. \quad (6.2)$$

Using a quantum loop expansion it was shown that the logarithmic integral of the spin-dependent photoabsorption cross section $\int_{\omega_{th}}^{\infty} \frac{d\omega_{\gamma}}{\omega_{\gamma}} \Delta\sigma^{Born}(\omega_{\gamma})$ vanishes for any $2 \rightarrow 2$ SM process $\gamma a \rightarrow bc$ in the classical, tree-graph approximation [31]. Here $\Delta\sigma = \sigma_{++} - \sigma_{+-}$ is the difference between the photoabsorption cross section for parallel and antiparallel photon and target helicities. A mean value theorem then implies that there must be a center of mass energy where the polarization asymmetry possesses a zero. The position of the zero may be determined with sufficient precision to constrain the anomalous couplings of the W to better than the 1% level at 95% CL [31]. Figure 6 shows the polarization asymmetry (6.2) for two different angular cuts as a function of energy. Radiative corrections shift the position of zero at about 280 GeV for the angular cut $10^{\circ} < \theta^{\pm} < 170^{\circ}$ (250 GeV for $30^{\circ} < \theta^{\pm} < 150^{\circ}$) to a lower energy by about 10 GeV. The dip from the 300 GeV Higgs boson is clearly seen. The corrections to the polarization asymmetry are of the order of $5 \div 10\%$ (outside the region near the crossing point) and so should necessarily be taken into account in realistic determinations of the precise constraints on the anomalous couplings of the W .

The most efficient way to experimentally constrain the anomalous couplings of the W -boson requires the extraction of the W^{\pm} spin-density matrix and the W^+ , W^- spin correlations from future data [11, 15, 32]. The polarization properties of the single W^+ (or W^-) decays are described

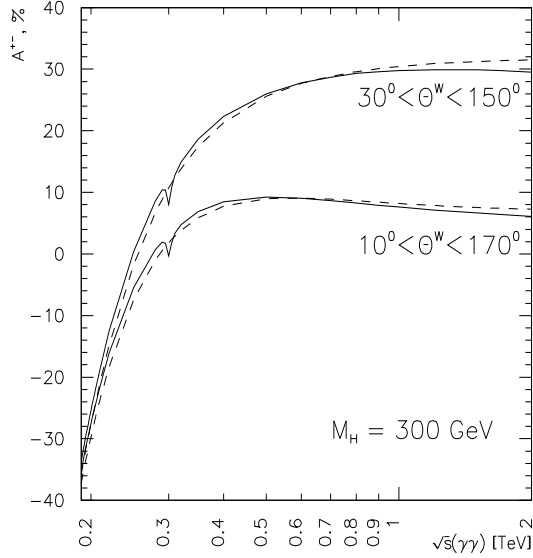


Fig. 6. Polarization asymmetry as a function of the center-of-mass energy. Dashed line is Born asymmetry and solid curve is the asymmetry with account of the radiative corrections.

by the single-particle density matrices

$$\begin{aligned} \rho_{\lambda_3 \lambda'_3 W^+}^{\lambda_1 \lambda_2}(\theta^+) &\propto \sum_{\lambda_4} \mathcal{M}_{\lambda_1 \lambda_2 \lambda_3 \lambda_4}(\gamma\gamma \rightarrow W^+ W^-) \mathcal{M}_{\lambda_1 \lambda_2 \lambda'_3 \lambda_4}^*(\gamma\gamma \rightarrow W^+ W^-) dPS^{(2)} \\ &+ \sum_{\lambda_4, \lambda_5} \int \mathcal{M}_{\lambda_1 \lambda_2 \lambda_3 \lambda_4 \lambda_5}(\gamma\gamma \rightarrow W^+ W^- \gamma) \mathcal{M}_{\lambda_1 \lambda_2 \lambda'_3 \lambda_4 \lambda_5}^*(\gamma\gamma \rightarrow W^+ W^- \gamma) dPS^{(3)}, \end{aligned} \quad (6.3)$$

here θ^+ is the W^+ production angle in the c.m.s. The normalization is

$$\sum_{\lambda_3, \lambda'_3} \rho_{\lambda_3 \lambda'_3 W^+}^{\lambda_1 \lambda_2}(\theta^+) = 1. \quad (6.4)$$

In Figures 7–9 we show the W^+ density-matrix elements (6.3) at the $\gamma\gamma$ center-of-mass energy of 500 GeV. Also the relative corrections with respect to the tree-level values are shown. Since off-diagonal matrix elements for equal initial photon helicities vanish at the tree-level, no relative corrections are given for these in the Figure 7. The imaginary parts shown in the Figure 9 also first appear at the one-loop level. Corrections to the dominant matrix elements are always less than 1%. The corrections to the subdominant matrix elements or to the dominant ones at the angles where they are suppressed are quite large.

7. Conclusions

The high energy laser induced $\gamma\gamma$ collider will be a real W factory and an ideal laboratory for precision tests on anomalous W interactions. The theoretical predictions for W pair production,

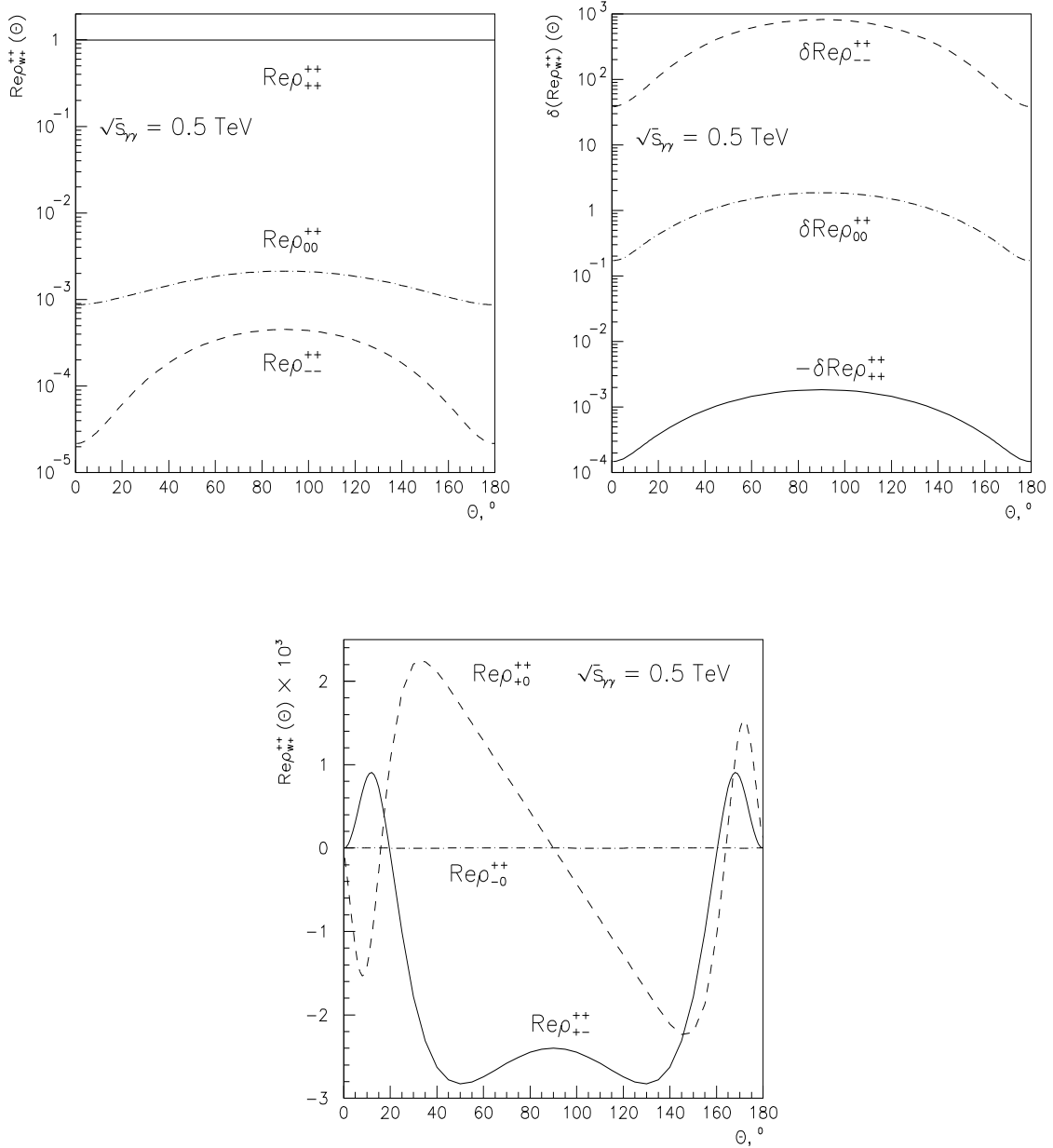


Fig. 7. The dependence on the production angle of the corrected single-particle density matrix elements and relative corrections for equal initial photons helicities $\lambda_1 = \lambda_2 = 1$.

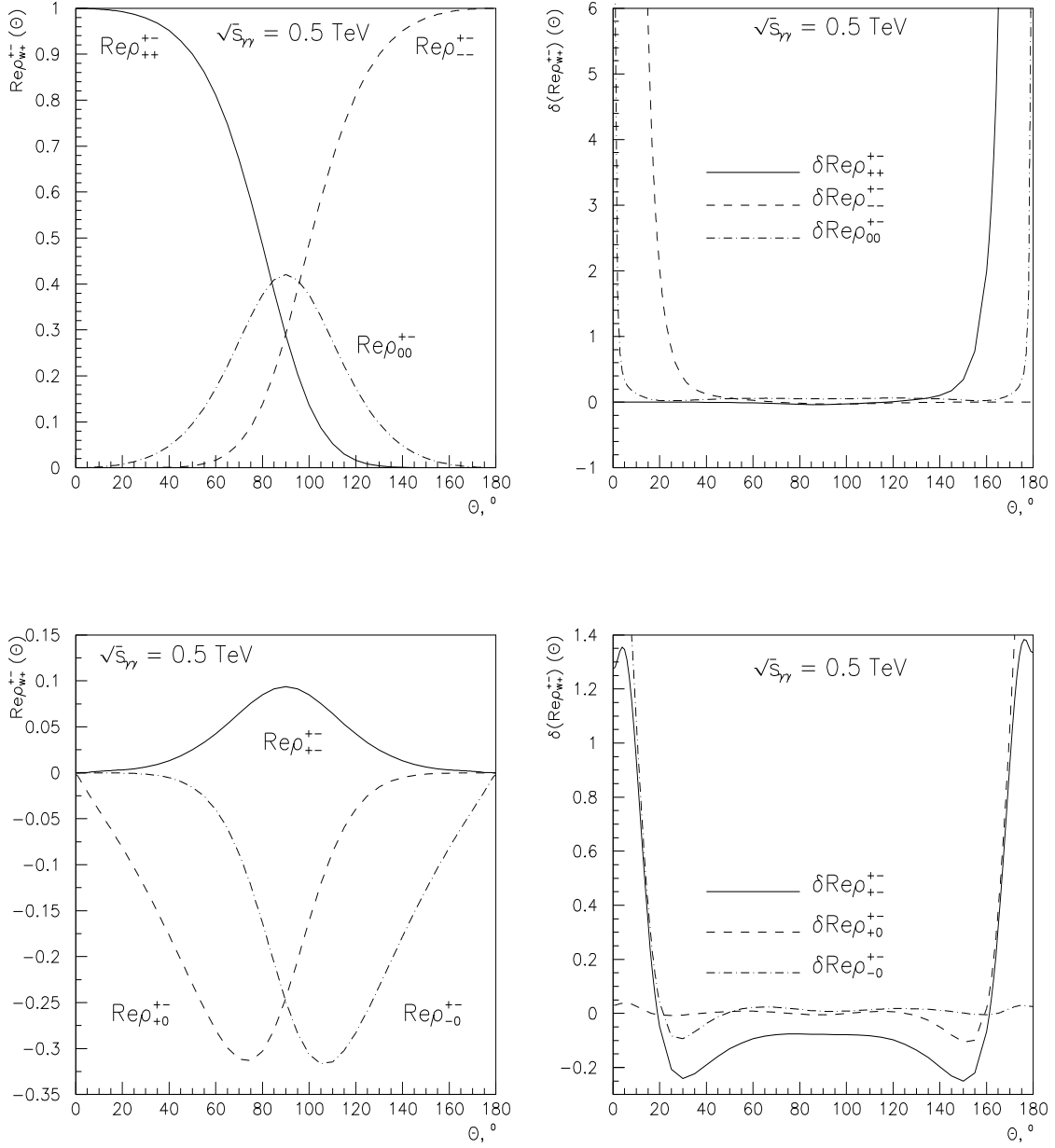


Fig. 8. The dependence on the production angle of the corrected single-particle density matrix elements and relative corrections for opposite initial photons helicities $\lambda_1 = -\lambda_2 = 1$.

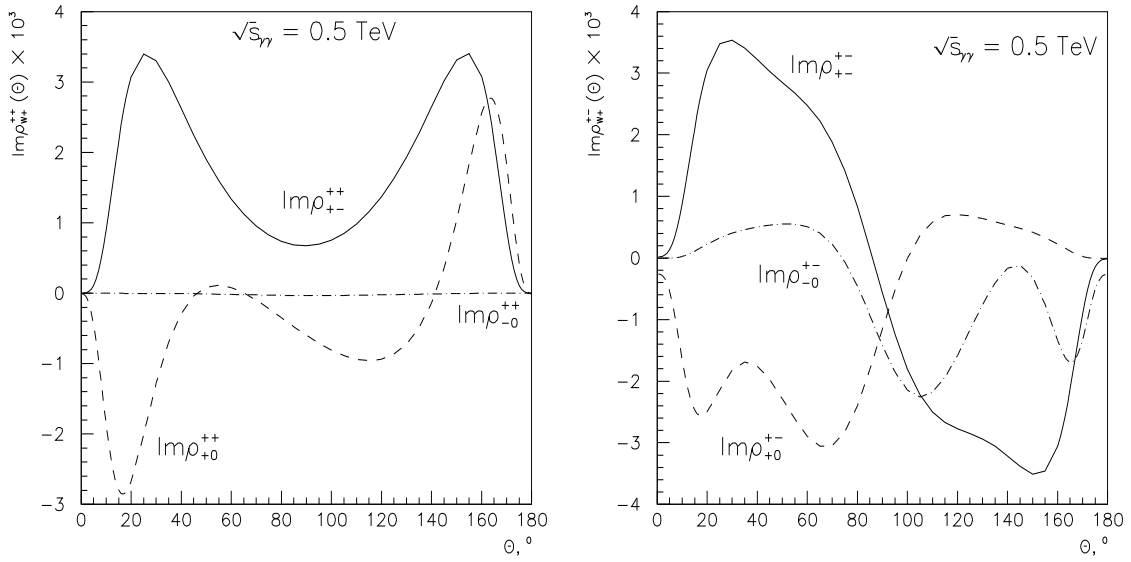


Fig. 9. The dependence on the production angle of the imaginary parts of the single-particle density matrix elements.

including complete electroweak $\mathcal{O}(\alpha)$ SM radiative corrections, are obtained with very little theoretical uncertainty at least for energies below 1 TeV. It is absolutely necessary to take them into account for precise measurements of the W properties.

Of course, searches for a new interactions will be the most interesting part of future experiments with W pair production. However, it is worth mentioning that WW production in photon-photon collisions should also qualify as a good $\gamma\gamma$ luminosity monitor [11, 13, 33]. As the interaction region in photon-photon collisions is quite complicated [1–3], it will be extremely important to measure the $\gamma\gamma$ differential luminosity and reconstruct the polarized photon spectra. In fact, one can imagine that the reaction $\gamma\gamma \rightarrow W^+W^-$ could be used both to uncover new physics and to calibrate luminosity. Indeed, anomalies would affect longitudinal and central W 's, while to measure luminosity one would use most copiously produced transverse and forward/backward W 's. Moreover, the analysis of Section 5 of the leading heavy Higgs boson and top-quark contributions shows, that the dominating cross sections of forward/backward transverse W_TW_T pair production are essentially insensitive to the details of new physics. Table 2 shows that radiative corrections for forward W scattering are quite small even at 2 TeV.

From the other side, as corrections for the total cross section in the central region are as large as $-(20 \div 40)\%$ at 2 TeV, a very relevant question relates to the size of the higher loop corrections. As the structure of leading corrections at high energies is known to have Regge form, one can imagine that at very high energies it would be possible to experimentally study the reggeization properties of massive weak bosons which are a unique feature of non-abelian spontaneously broken gauge theory.

Acknowledgements

This work was supported in part by the Alexander von Humboldt Foundation and the Russian Foundation for Basic Research grant 96-02-19-464.

References

- [1] I.F. Ginzburg, G.L. Kotkin, V.G. Serbo and V.I. Telnov, *Pis'ma ZhETF* **34** (1981) 514; *Nucl. Instr. and Meth.* **205** (1983) 47; I.F. Ginzburg, G.L. Kotkin, S.L. Panfil, V.G. Serbo and V.I. Telnov, *Nucl. Instr. and Meth.* **219** (1984) 5; V.I. Telnov, *Nucl. Instr. and Meth.* **A355** (1995) 3.
- [2] V.E. Balakin and A.A. Sery, *Nucl. Instr. and Meth.* **A355** (1995) 157.
- [3] D.J. Schulte, 3rd Workshop e^+e^- Collisions at TeV Energies: the Physics Potential, Part D, DESY, Hamburg, Germany, August 30 – September 1, 1995, p. 463.
- [4] P.M. Zerwas, Proceedings of the *VIII Int. Workshop on Photon-Photon Collisions*, Shoresh (Jerusalem Hills) 1988; R. Najima, Proceedings, of the Workshop *Physics at TeV energy scale*, Tsukuba 1989, Report KEK-90-009, p. 112; I.F. Ginzburg, Novosibirsk Preprint TF-28-182, 1990; E. Boos, I. Ginzburg, K. Melnikov, T. Sack and S. Shichanin *Z. Phys.* **C56** (1992) 487; G. Jikia, *Nucl. Phys.* **B405** (1993) 24; O.J.P. Éboli, M.C. Gonzalez-Garcia, F. Halzen, and D. Zeppenfeld, *Phys. Rev.* **D48** (1993) 1430; D.L. Borden, D.A. Bauer, D.O. Caldwell, *Phys. Rev.* **D48** (1993) 4018; J.F. Gunion and H.E. Haber, *Phys. Rev.* **D48** (1993) 5109; M.S. Berger, *Phys. Rev.* **D48** (1993) 5121; D.A. Dicus and C. Kao, *Phys. Rev.* **D49** (1994) 1265; D. L. Borden, V. A. Khoze, W. J. Stirling, and J. Ohnemus, *Phys. Rev.* **D50** (1994) 4499; J.F. Gunion, J.G. Kelly and J. Ohnemus, *Phys. Rev.* **D51** (1995) 2101; M. Baillargeon, G. Belanger and F. Boudjema, *Phys. Rev.* **D51** (1995) 4712; B. Kamal, Z. Merebashvili and A.P. Contogouris, *Phys. Rev.* **D51** (1995) 4808; V.A. Khoze, Proceedings of the *10th Workshop on Photon-Photon Collisions*, Sheffield, England, 8–13 April 1995; I. Watanabe, Proceedings of the Workshop Physics and Experiments with Linear e^+e^- Colliders, Morioka, Japan, September 8–12, 1995; G. Jikia and A. Tkabladze, *Phys. Rev.* **D54** (1996) 2030; D. Choudhury and M. Krawczyk, Report MPI-PTH-96-46, July 1996, hep-ph/9607271.
- [5] E.E. Boos, G.V. Jikia, *Phys. Lett.* **B275** (1992) 164.
- [6] H. Veltman, *Z. Phys.* **C62** (1994) 235.
- [7] A. Denner, R. Schuster, S. Dittmaier, *Phys. Rev.* **D51** (1995) 4738.
- [8] D.A. Morris, T.N. Truong and D. Zappala, *Phys. Lett.* **B323** (1994) 421.
- [9] E. Yehudai, *Phys. Rev.* **D44** (1991) 3434.
- [10] S.Y. Choi and F. Schrempp, *Phys. Lett.* **B272** (1991) 149.
- [11] M. Baillargeon, G. Belanger, and F. Boudjema, Proc. of the “*Two-Photon Physics from DAΦNE to LEP200 and Beyond*”, 2-4 February 1994, Paris.
- [12] G. Bélanger and F. Boudjema, *Phys. Lett.* **B288** (1992) 210.

- [13] M. Baillargeon and F. Boudjema *Phys. Lett.* **B317** (1993) 371.
- [14] F.T. Brandt, O.J.P. Éboli, E.M. Gregores, M.B. Magro, P.G. Mercadante and S.F. Novaes, *Phys. Rev.* **D50** (1994) 5591.
- [15] M. Baillargeon, G. Bélanger, F. Boudjema and G. Jikia, Proceedings of the 3rd Workshop e^+e^- Collisions at TeV Energies: the Physics Potential, Part D, DESY, Hamburg, Germany, August 30 – September 1, 1995, p. 511.
- [16] G. Jikia, Proceedings of the Workshop Physics and Experiments with Linear e^+e^- Colliders, Morioka, Japan, September 8–12, 1995.
- [17] F. Boudjema, in Physics and Experiments with Linear e^+e^- Colliders, Waikoloa, Hawaii, 1993, Ed. F.A. Harris *et al.*, World Sci., vol. II, p. 712; F. Boudjema, in Physics and Experiments with Linear e^+e^- Colliders, Morioka, Japan, September 8–12, 1995.
- [18] A. Denner, S. Dittmaier, and R. Schuster, *Nucl. Phys.* **B452** (1995) 80; Proceedings of the 3rd Workshop e^+e^- Collisions at TeV Energies: the Physics Potential, Part D, DESY, Hamburg, Germany, August 30 – September 1, 1995, p. 233; Report BI-TP 96/03, WUE-ITP-96-001, hep-ph/9601355.
- [19] G. Jikia, *Nucl. Phys.* **B437** (1995) 520.
- [20] K.-i. Aoki, Z. Hioki, R. Kawabe, M. Konuma and T. Muta, *Suppl. Prog. Theor. Phys.* **73** (1982) 1; M. Böhm, H. Spiesberger and W. Hollik, *Fortschr. Phys.* **34** (1986) 687.
- [21] R.G. Stuart, *Phys. Lett.* **B272** (1991) 353.
- [22] J.A.M. Vermaasen, Symbolic Manipulation with FORM, published by CAN, Kruislaan 413, 1098 SJ Amsterdam, 1991, ISBN 90-74116-01-9.
- [23] G. 't Hooft and M. Veltman, *Nucl. Phys.* **B153** (1979) 365.
- [24] G.J. van Oldenborgh and J.A.M. Vermaasen, *Z. Phys.* **C46** (1990) 425.
- [25] G.J. van Oldenborgh, *Comput. Phys. Commun.* **66** (1991) 1.
- [26] S. Kawabata, *Comput. Phys. Commun.* **88** (1995) 309.
- [27] T. Kinoshita, *J. Math. Phys.* **3** (1962) 650; T.D. Lee and M. Nauenberg, *Phys. Rev.* **133B** (1964) 1549.
- [28] V.S. Fadin, E.A. Kuraev and L.N. Lipatov, *Phys. Lett.* **B60** (1975) 50; L.N. Lipatov, *Sov. J. Nucl. Phys.* **23** (1976) 338; E.A. Kuraev, L.N. Lipatov and V.S. Fadin, *Sov. Phys. JETP* **44** (1976) 443.
- [29] B.M. McCoy and T.T. Wu, *Phys. Rev.* **D13** (1976) 1076; C.Y. Lo and H. Cheng, *Phys. Rev.* **D13** (1976) 1131.
- [30] Particle Data Group, *Phys. Rev.* **D54** (1996) 1.
- [31] S.J. Brodsky and I. Schmidt, *Phys. Lett.* **B351** (1995) 344; S.J. Brodsky, T.G. Rizzo and I. Schmidt, *Phys. Rev.* **D52** (1995) 4929.

- [32] M. Bilenky, J.L. Kneur, F.M. Renard and D. Schildknecht, *Nucl. Phys.* **B409** (1993) 22.
- [33] Y. Yasui, I. Watanabe, J. Kodaira and I. Endo, *Nucl. Instr. Meth.* **A335** (1993) 385.